American Journal of Pathology, Vol. 144, No. 2, February 1994

Dose-Dependent Tolerance to Ozone

I. Tracheobronchial Epithelial Reorganization in Rats After 20 Months' Exposure

Charles G. Plopper,*† Fung-Ping Chu,* Carole J. Haselton,* Janice Peake,† James Wu,* and Kent E. Pinkerton†

From the Department of Anatomy and Cell Biology, School of Veterinary Medicine, and California Regional Primate, Research Center, †University of California, Davis, California*

Two salient features of the pulmonary response to reactive oxidant air pollutants such as ozone are the heterogeneity of response by site within the respiratory tract and the development of tolerance to injury with repeated exposure. The purpose of this study was to establish whether the development of tolerance to long-term exposure is associated with changes in the tracheobronchial epithelium. Male F344-N rats were exposed to 0, 0.12, 0.5, or 1.0 ppm ozone 6 hours/day for 5 days/week for 20 months and killed 1 week post-exposure. Samples for light microscopic morphometry were obtained by microdissection from each infusion-fixed trachea and left lung lobe and included: 1) a cranial bronchus with short path length (generation no. 4 to 5) and small diameter; 2) a central bronchus with short path length (generation no. 4 to 5) and large diameter; and 3) a caudal bronchus with long path length (generation no. 10 to 12) and small diameter. In addition, three sites within the central acinus were examined from cranial, central, and caudal regions. These sites included terminal bronchiole, 0.5 to 1 mm proximal to terminal bronchiole and bronchiolarized alveolar duct. Intraepithelial mucin storage (AB/PAS-positive material quantified by image analysis) within the trachea decreased with dose. Mucin storage was unchanged in the central bronchus, increased threefold with dose in the caudal bronchus, and was six times higher in the cranial bronchus at 1.0 ppm ozone. Epithelial composition was unchanged in trachea or any bronchi; however, we noted a significant dose-dependent increase in nonciliated cell mass and volume fraction in terminal bronchioles in all three regions. There was also a significant increase in nonciliated cell mass in the bronchiolarized alveolar ducts. Bronchiolar nonciliated cells were identified greater than fourfold further into alveolar ducts in 1.0 ppm exposed than in 0 ppm animals. Nonciliated cells occurred almost 200 μm deeper into alveolar ducts in cranial regions than in caudal regions. We conclude: 1) that the development of tolerance to injury produced by long-term exposure to ozone involves changes in airway epithelium and 2) that these changes are site specific and involve alterations in both secretory activity and cellular composition. (Am J Pathol 1994, 144:404–421)

As one of the primary interfaces between the organism and the environment, the mammalian respiratory system is a target for various toxic gases and particles. In the case of the oxidant air pollutant ozone, the response to exposure has at least two distinct features. First, the acute response is not uniform throughout the tracheobronchial airway tree: the injury is oriented toward the epithelium and is highly focal and site specific. Second, the acute injury associated with short-term exposure is significantly attenuated by repeated, long-term exposure. The mechanism by which the epithelial cells develop tolerance to further injury via ozone or other oxidant gases is poorly understood. Previous studies focusing on the centriacinar region in the rat, a primary site of injury and inflammation associated with short-term exposure, have found epithelial reorganization, metaplasia, and alveolar duct bronchiolarization after long-term expo-

Supported in part by NIEHS grant ES00628.

Accepted for publication October 7, 1993.

Address reprint requests to Dr. Charles G. Plopper, Department of Anatomy and Cell Biology, School of Veterinary Medicine, University of California, Davis, CA 95616.

sure (90 day).[1–4] Bronchiolarization involves the formation of cuboidal epithelium in proximal alveolar ducts after long-term (up to 90 days) exposure. More recently, we have examined this region in animals exposed for near lifetime (20 months) and demonstrated the presence of Clara cell secretory protein, a marker of differentiated function in Clara cells, in the nonciliated epithelial cells lining these bronchiolarized alveolar ducts.[5] We have also reported that both the epithelial injury and the inflammation associated with the acute response to initial exposure vary by position within the airway tree.[6] Schlesinger et al[7] suggest that variability by airway size may also occur with the chronic response to long-term exposure. The purpose of this study was to establish whether development of tolerance to long-term ozone exposure is associated with changes in the epithelium lining tracheobronchial airways, including various regions of the centriacinus, and whether these changes were related to position within the airway tree or the centriacinus. We exposed rats to ambient concentrations (0.12, 0.5, 1.0 ppm) of ozone or to filtered air for near lifetime (20 months) and evaluated changes in intraepithelial glycoconjugates stored within the proximal intrapulmonary bronchi and trachea and assessed epithelial cell density and composition in the airways.

Materials and Methods

Animals and Ozone Exposure

Male Fischer 344-N rats were obtained from Simonsen Laboratories (Gilroy, CA) at 4 to 5 weeks of age. Animals were randomly assigned to ozone exposure or control groups after a 10- to 14-day quarantine period. Animals were housed in modified Hazelton 2000 inhalation chambers and exposed to either ozone or filtered air for 6 hours/day (between 7:30 a.m. and 5:30 p.m.) 5 days/week for 20 months. Exposure to ozone was performed at Battelle, Pacific Northwest Laboratories (Richland, WA) as part of a collaborative, multilevel study with the National Toxicology Program (NTP) and Health Effects Institute (HEI) to examine the long-term effects of ozone. Due to the scope of the NTP/HEI study and the large number of animals involved, the animals that formed the basis of this study were received from a total of three different exposure chambers for each ozone concentration and from three chambers for filtered air. The animals were chosen from different chambers because they were exposed as part of a larger bioassay study and were made available on the condition that they share chamber space. Animals were chosen by a strictly randomized scheme. The animals were free of respiratory disease, as judged by the testing of sentinel animals from each chamber throughout the exposure period and at the end of the study. The average temperature range (±SD) within the exposure chambers over the course of the study was 23.9 to 24.4 (±0.7) C; the relative humidity range was 57.1 to 60.2 (±7.3)%.

Ozone was generated by corona discharge using an OREC model 03V5-0 ozonator (Ozone Research and Equipment Corporation, Phoenix, AZ) with 100% oxygen. Ozone concentration in each chamber was monitored by a multiplexed Dasibi model 1003-AH ultraviolet spectrophotometric analyzer (Dasibi Environmental Corporation, Glendale, CA). Calibration of the monitor was accomplished by comparison with a chemical-specific calibrated (neutral-buffered potassium iodide method) monitor simultaneously sampling the exposure chambers. The target concentrations for ozone were 0.00 ppm for the control chambers and 0.12, 0.5, and 1.00 ppm for the ozone chambers. The actual exposure concentration over the course of the study in the control chambers was less than 0.002 ppm (below the limit of detection) and 0.12 (±0.01), 0.51 (±0.02), and 1.01 (±0.05) ppm (mean ± SD) in the ozone chambers. To determine concentration uniformity, measurements were periodically made at 12 levels or locations in each chamber. Ambient ozone was removed from all chambers using a potassium permanganate filter. Charcoal and HEPA filters were used to further filter air entering the chambers. At the end of the 20-month exposure, all animals were held for 1 week before death to emphasize permanent, nontransient changes in the lungs.

Lung Fixation and Processing for Microscopy

For this study, four animals from the control group and four animals from each of the exposure groups were randomly selected for evaluation. Animals were killed with an overdose of Na pentobarbital. The lungs were collapsed by diaphragmatic puncture and fixed *in situ* by intratracheal instillation of 2% glutaraldehyde in cacodylate buffer (pH 7.4, 350 mOsm) for 15 minutes at 30 cm fixative pressure.[8] The fixed lungs were removed by thoracotomy and stored in the same fixative until processing for immunohistochemistry, histochemistry, light microscopy, and scanning electron microscopy. The fixed lungs were trimmed of all mediastinal contents and the lung volumes measured by

fluid displacement. Regions of left lung lobe were selected for complementary histochemistry and high resolution light microscopy.

Beginning with the trachea, airways were dissected along their long axes to approximately the level of the terminal bronchiole.[8] The dissections were done with the aid of a Wild M8 dissecting microscope (Wild Heerbrugg Instruments, Farmingdale, NY) and fiberoptic illumination. The areas selected for study are illustrated in Figure 1 and are identified as the cranial, central, and caudal regions. As summarized in Table 1, the cranial region

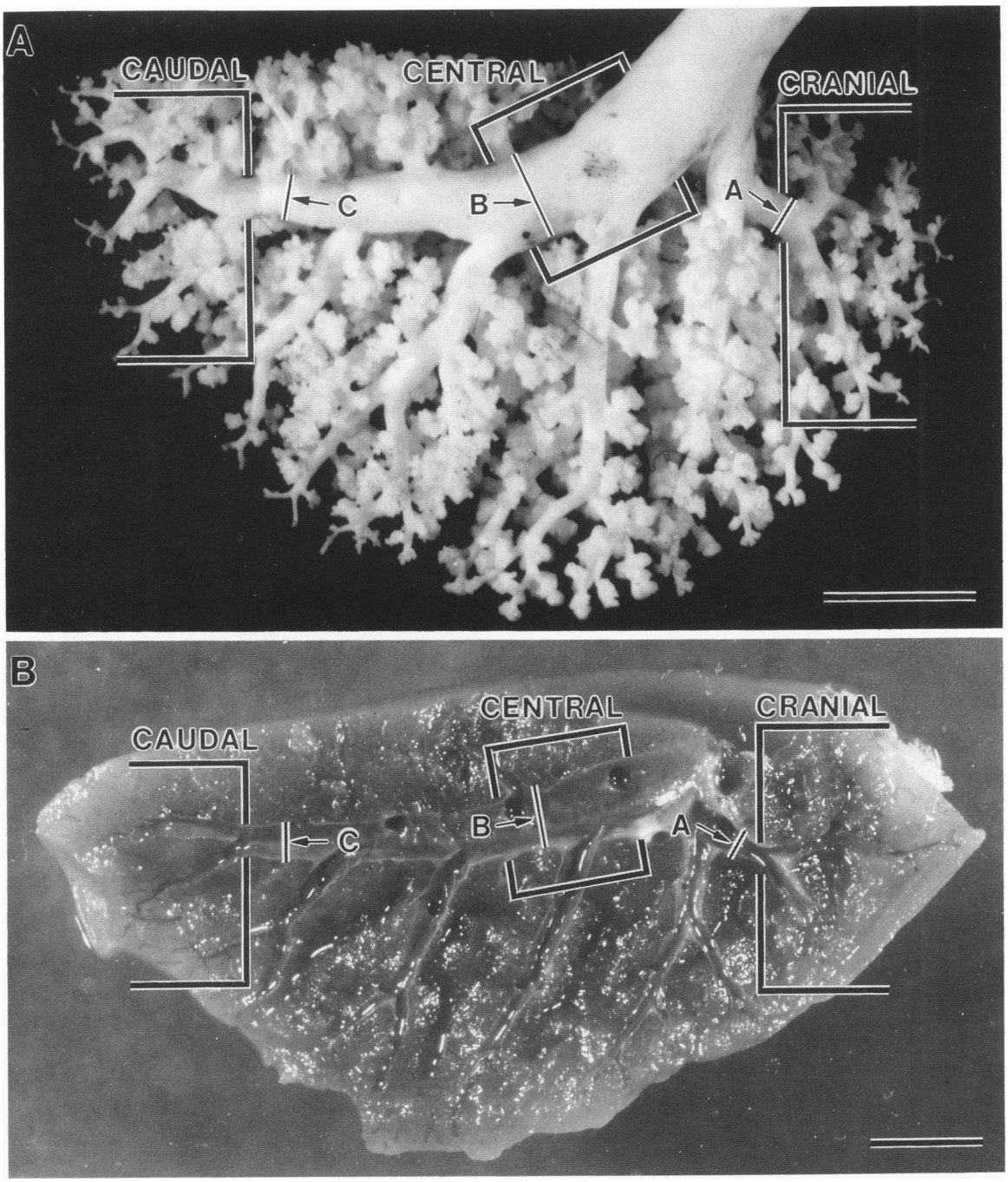

Figure 1. *Location of tissue samples taken from rat lung.* (**A**)*: Silicone cast of the tracheobronchial airway tree from the left lobe of a rat. Lung casts served to standardize sampling. Samples of terminal bronchiole-alveolar duct junctions were taken from the three regions* (*cranial, central, and caudal*) *indicated. The letters and arrows indicate the precise locations from which samples of intrapulmonary conducting airways were taken. Bar = 4 mm.* (**B**)*: Mediastinal half of a fixed, microdissected rat lung. Note how closely the pathways and sampling regions match the silicone cast shown above. Bar = 4 mm.*

Table 1. *Characteristics of Airway Specimens*

Airway	Generation number	Path length from carina (mm)	Cumulative branch angle (°)	Diameter (mm)
Distal trachea	0	N/A	N/A	3.3 ± 0.1
Lobar bronchus	1	6.7 ± 0.1	15 ± 0	2.8 ± 0.1
Cranial region bronchus	4–5	14.0 ± 1.2	140 ± 15	0.7 ± 0.0
Central acinus	8–10	14.0 ± 1.2	225 ± 21.8	—
Central region bronchus	4–5	13.7 ± 1.1	8.3 ± 5.8	2.4 ± 0.1
Central acinus	6–7	11.2 ± 0.3	50 ± 8.7	—
Caudal region bronchus	10–12	20.2 ± 0.4	30.0 ± 8.6	1.0 ± 0.1
Central acinus	15–16	22.3 ± 0.3	30.0 ± 8.6	—

N/A, not applicable.

included a medium-sized conducting airway with a short path length, a large cumulative angle of change in the path direction, and a relatively small diameter. The cranial centriacinar regions were selected from the acini supplied by this bronchial pathway. The conducting airway selected from the central region had the same number of generations of branching as that of the cranial region but was much larger in diameter and was part of the axial pathway for conducting airways in the left lobe. The airway selected from the caudal region had a much greater path length and approximately the same diameter as that of the cranial bronchus; however, the angle of deviation was much less in the caudal airway.

Identifying airway location during dissection was facilitated by using silicone casts prepared from the lungs of three 4- to 5-month-old male Fischer 344-N rats. Each cast was prepared according to a modified saline displacement casting procedure in which silicone rubber (Dow Corning Silastic 734 RTV, Dow Corning Corporation, Midland, MI) is injected into the trachea at 25 m pascal (cm of water) positive pressure. After curing for 2 days, the silicone-filled lungs were removed from the thorax and boiled in 1 N sodium hydroxide to remove the lung tissue. Casts were trimmed to reveal airways from the major bronchus to the level of the terminal bronchioles. The path length and cumulative branch angle of each airway was measured directly from the casts.

The rat lung has a monopodial form of airway branching in which a major and minor daughter airway arise from each parent airway. A labeling system devised by Phalen et al[9,10] exploits this unique arrangement and uses a binary numbering scheme to label all sequential major airways as "1" and all minor airways as "0." Beginning at the trachea (designated as 1), the classification of each new airway generation is added to give a unique branching history for each pathway. These branching histories were easily and reliably determined from the lung casts and were used as guides to ensure that dissections in the fixed, wet lungs followed identical pathways to each region in every lung. Table 1 summarizes the branching history, generation number, path length, diameter, and cumulative branch angle for each airway followed. The most distal airway(s) revealed by microdissection were usually two to four generations from the terminal bronchioles. Blocks of tissue approximately 1.5 × 1.5 × 0.4 mm in size were cut in a plane perpendicular to the axis of the most distal dissected airway to isolate parenchymal tissue arising from each dissected pathway.

Portions of the dissected left lung were embedded in glycolmethacrylate. One-micron sections were cut with glass knives on a JB4 microtome. Serial and serial-step sections were stained with Alcian blue/periodic acid Schiff (pH 2.5) or toluidine blue (0.5% in 1% borate).

For the cranial and caudal regions, blocks were removed, embedded as large blocks, and the bronchiole-alveolar duct junctions (BADJ) were isolated by the methods of Pinkerton et al[5]. Briefly, tissue slices (approximately 2 × 4 × 6 mm in size) were postfixed in 1% osmium tetroxide in Zetterquist's buffer, followed sequentially by 1% tannic acid and 1% uranyl acetate in maleate buffer, dehydrated in ethanol and propylene oxide and embedded in either Epon 812 or Araldite 502. Centriacinar regions were isolated by cutting the entire tissue block into slices approximately 0.3 to 0.4 mm thick. Each slice was examined under a dissecting microscope to identify BADJs in longitudinal profile. The criterion for selection was a symmetrical pair of alveolar ducts arising from a single terminal bronchiole. Isolations meeting this selection criterion consistently contained alveolar duct paths in longitudinal profile that extended two to four generations beyond the BADJ. Selected isolations were remounted on BEEM capsules and sectioned at a

thickness of 0.5 μ with glass knives. Sections were stained with toluidine blue (0.5% in 1% borate buffer).

Morphometry

The thickness and relative abundance of conducting airway epithelial cells were evaluated by procedures that are discussed in detail elsewhere.[11–13] All measurements were made using high resolution light microscopy (40× objective and 0.5- to 1.0-μ sections). Measurements were made from video images captured with a DAGE MTI video camera (Michigan City, IN) mounted on an Olympus BH-2 microscope, which was interfaced with a Macintosh IIci computer running IMAGE software. The analysis was performed using a cycloid grid overlay and software for counting points and intercepts (Stereology Toolbox, Davis, CA) (see references 11 and 12 for detailed description of grids and counting procedures). The volume densities (V_v) of three categories of cells (nonciliated, ciliated, and basal) were determined by point counting and were calculated using the formula:

$$V_v = P_p = P_n/P_t$$

where P_p is the point of fraction P_n, the number of test points hitting the structure of interest, divided by P_t, the total points hitting the reference space (epithelium). The surface area of epithelial basement membrane per reference volume (S_v) was determined by point and intercept counting and was calculated using the formula:

$$S_v = 2\ I_0/L_r$$

where I_0 is the number of intercepts with the object (epithelial basal lamina) and L_r, is the length of test line in the reference volume (epithelium). To determine thickness of the epithelium, a volume per unit area of basal lamina (μ^3/μ^2) was then calculated using the formula for arithmetic mean thickness (τ):

$$\tau = V_v/S_v$$

Abundance of stored mucin was estimated using the thresholding and particle counting function of the IMAGE software to measure the area of AB/PAS-positive material in a defined area of epithelial profile and the percentage of the epithelium occupied by AB/PAS-positive material calculated. The volume of AB/PAS material per unit area of basal lamina was determined by multiplying the percentage of AB/PAS-positive material in the epithelium by the thickness of epithelium determined at the site.[11,12]

For each bronchus and the trachea, four fields were evaluated. Fields were selected at random by dividing the cross-section of the airway into four quadrants, choosing a random angle (between 0 and 90°) from a random number table and centering the field for evaluation on that angle. In the centriacinar region, a minimum of five centriacinar areas was used for each analysis. Figure 2 illustrates the positions of the areas sampled. Epithelium evaluated for the terminal bronchiole was defined as the epithelium just proximal to the first alveolar outpocketing. Epithelium defined as proximal bronchiole was obtained from a site contiguous with the terminal bronchiole but 0.5 to 1 mm more proximal. Samples of bronchiolarized epithelium in alveolar ducts were taken in the same centriacinar regions used for the terminal bronchiole measurements and included areas separated on either side by alveolar outpocketings. The extent of bronchiolarization into the alveolar duct in cranial and caudal regions of 0.0 and 1.0 ppm rats was determined as previously reported.[5]

Statistics

Values were calculated on a per animal basis from counts made on at least four fields per airway and were used to calculate the mean and SD for each exposure group. Differences between group values were assessed by analysis of variance and one-way regression analysis. Significance was determined by Scheffe's F-test as $P < 0.05$.[14]

Results

Trachea

Carbohydrate histochemical staining identified AB/PAS-positive material in the epithelium of the trachea (Figure 3). Most of the staining was confined to circular inclusions within the apices of nonciliated cells. These granules ranged in color from a purplish-pink to deep purple. There was little difference in the color range among different exposure groups. The primary intergroup differences were an apparent reduction in the abundance of secretory product within nonciliated cells and a reduction in the number of cells with AB/PAS-positive inclusions. There was a statistically significant difference between exposure groups in the amount of AB/PAS-positive mucin stored in the epithelium of the trachea (Table 2). There was approximately one-half

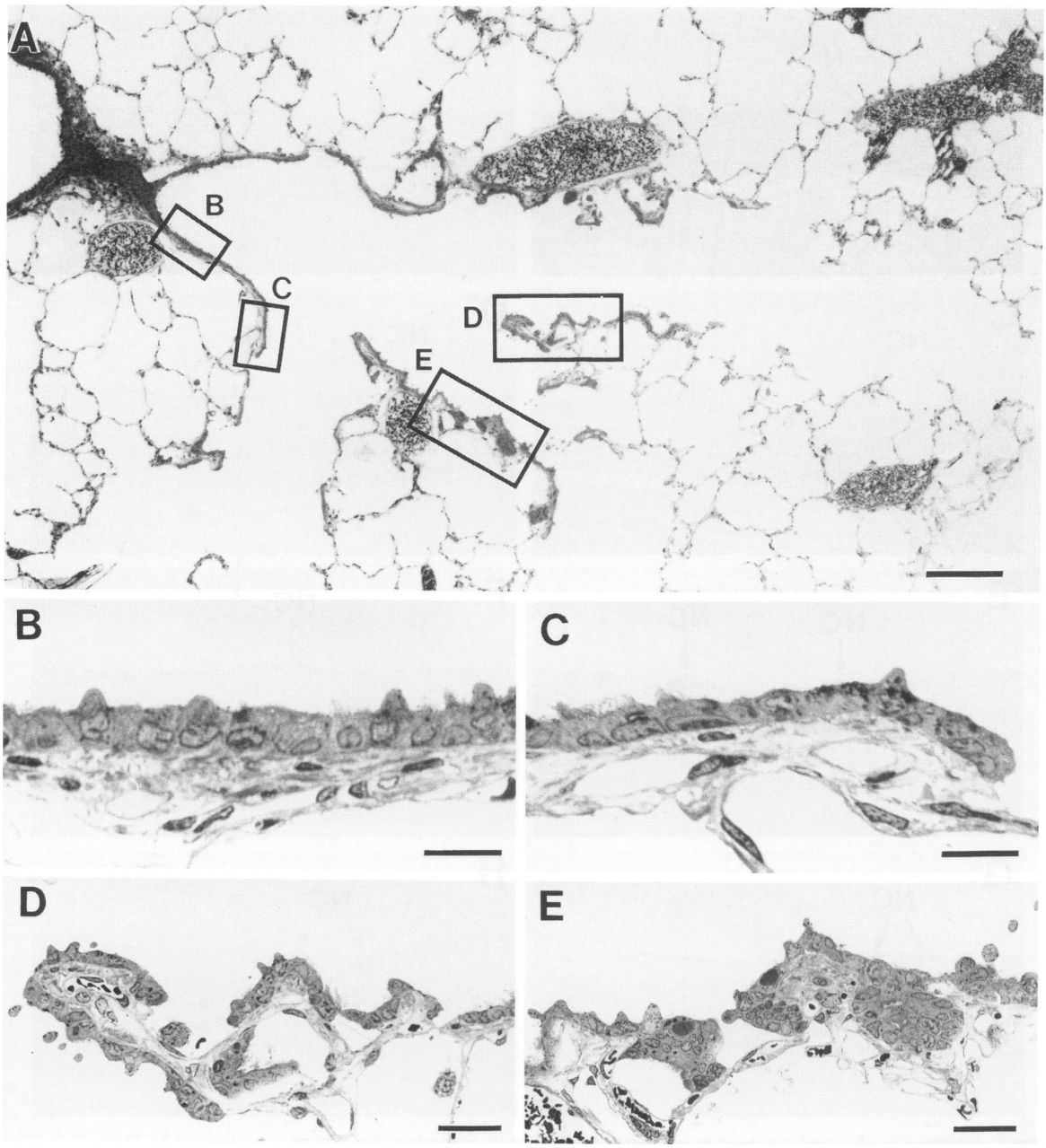

Figure 2. *Position and composition of regions analyzed within the terminal bronchiole-alveolar duct junction.* (**A**): *Epithelium representing distal bronchioles one generation proximal to the terminal bronchiole was sampled approximately 0.5 to 1.0 mm from the junction (box B). Centriacinar region from a rat exposed to 1.0 ppm ozone for 20 months. Epithelium from the terminal bronchiole was selected at the junction with the first alveolar duct (box C). Epithelium in the bronchiolarized alveolar duct was taken from bronchiolar epithelium clearly identified within the alveolar duct (boxes D and E). Bar = 150 μm.* (**B**): *Epithelial composition of the area in box B above. Bar = 15 μm.* (**C**): *Epithelial composition of the area in box C above. Bar = 15 μm.* (**D**): *Epithelial composition of the area in box D above. The epithelium in alveolar ducts lined both sides of interalveolar septa and in many cases appeared to be hyperplastic and metaplastic. Bar = 30 μm.* (**E**): *Epithelial composition of the area in box E above. Bar = 30 μm.*

as much material in the tracheas of animals exposed to 1.0 ppm ozone as in animals exposed to filtered air (Figure 4). This difference correlated with exposure concentration.

Compared with control animals, the histological appearance of epithelial cells lining the distal trachea was not appreciably different in rats exposed to 0.12 to 0.5 ppm ozone (Figure 5). The ciliated cells were easily discernible by their light cytoplasmic staining and appeared to have an abundance of cilia. Two categories of nonciliated cells were present. The secretory cell population extended from the basal lamina to the lumen and contained variable numbers of densely staining secretory

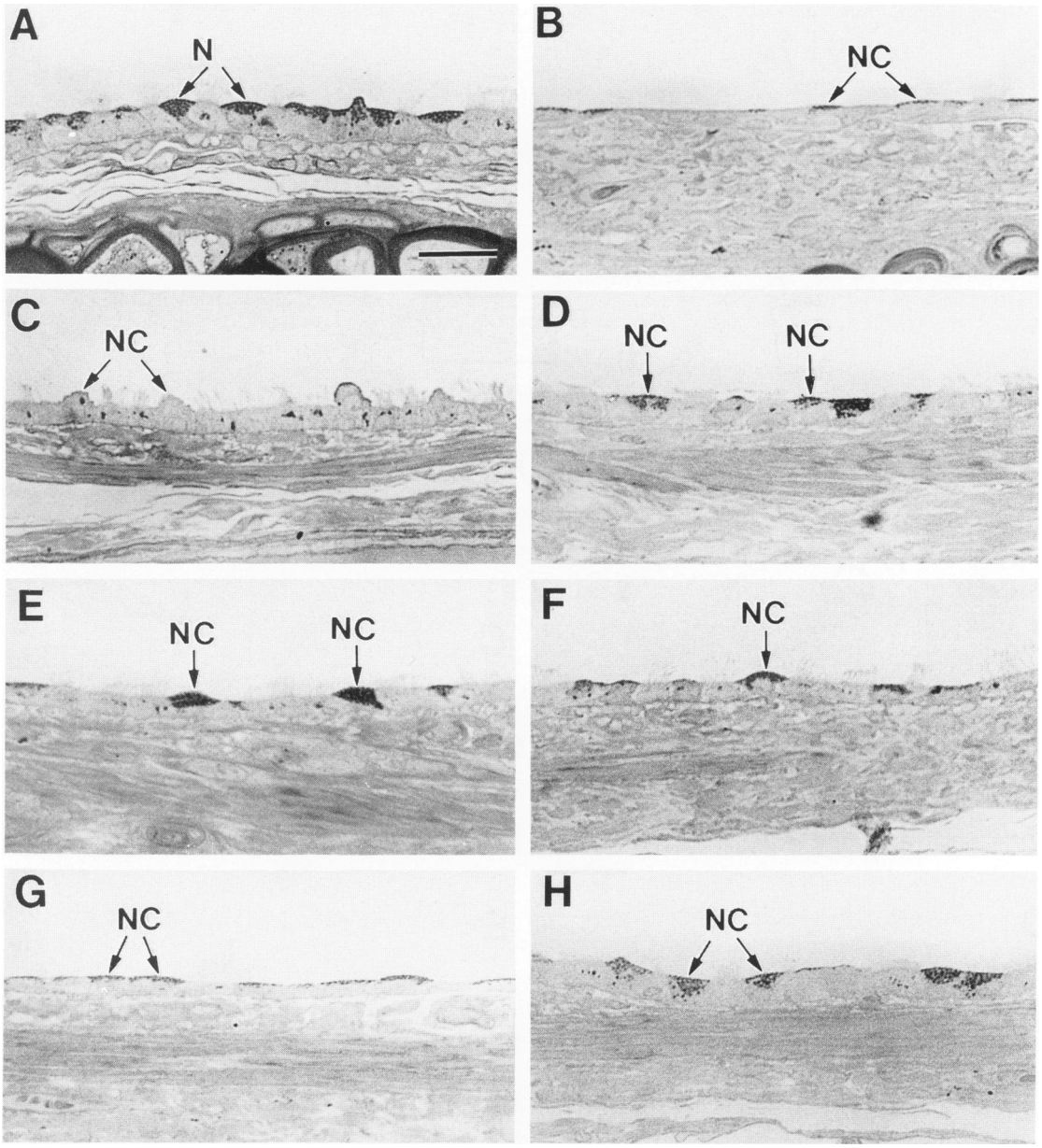

Figure 3. *Differences in glycoconjugate stored in nonciliated cells (NC) in the tracheobronchial airways of rats exposed for 20 months to filtered air* (left column) *or 1.0 ppm ozone (right column) (O_3). Alcian blue/periodic acid Schiff. Bar = 20 μm.* (**A,B**): *Trachea.* (**C,D**): *Cranial bronchus.* (**E,F**): *Central bronchus.* (**G,H**): *Caudal bronchus.*

granules. Basal cells were few and identified by the triangular-to-fusiform shape and distribution of the nucleus parallel to the basal lamina. In the animals exposed to 1.0 ppm ozone, there appeared to be a larger proportion of epithelium that was reduced in thickness compared with control specimens (Figure 5). There also appeared to be more nonciliated cells and fewer ciliated cells than in control animals. Morphometric assessment of the average thickness of the tracheal epithelium indicated that there was some reduction in epithelial thickness in the group exposed to 1 ppm ozone but due to the variability in different sites in all animals these differences were not statistically significant (Table 3). Nonciliated cells occupied a slightly larger percentage of the epithelial volume in exposed groups compared with control animals (Table 4); however, the variability was extremely high from group to group. There was no significant change in the absolute mass of nonciliated cells (Table 5). The remainder of the cells

Table 2. *Intraepithelial Mucin ($\mu m^3/\mu m^2$) Stored in Tracheobronchial Airways of Rats Exposed to Ozone for 20 Months*

Airway	Region	Ozone concentration (ppm) 0.0	0.12	0.5	1.0
Distal trachea		0.70 ± 0.19*	+0.59 ± 0.09*	+0.45 ± 0.21*	+0.36 ± 0.14*
Bronchus	Cranial	0.05 ± 0.07	0.01 ± 0.01	0.03 ± 0.04	0.31 ± 0.08†
Bronchus	Central	0.19 ± 0.07	0.26 ± 0.15	0.17 ± 0.09	0.21 ± 0.12
Bronchus	Caudal	0.09 ± 0.10*	0.14 ± 0.07*	0.15 ± 0.13*	0.27 ± 0.11*†

* Dose response $P < 0.05$ based on regression analysis.
† $P < 0.05$ compared with 0.0 ppm.

Table 3. *Total Epithelial Thickness (μm) in Tracheobronchial Airways of Rats Exposed to Ozone for 20 Months*

Airway	Region	Ozone concentration (ppm) 0.0	0.12	0.5	1.0
Distal trachea		7.60 ± 1.66	7.70 ± 2.73	7.99 ± 2.74	5.73 ± 1.43
Bronchus	Cranial	6.01 ± 1.31	6.54 ± 1.66	7.15 ± 2.15	6.87 ± 1.01
Bronchus	Central	5.30 ± 1.09	6.43 ± 1.74	5.13 ± 0.51	5.21 ± 1.32
Bronchus	Caudal	7.82 ± 2.32†	7.71 ± 1.66†	6.99 ± 0.52†	5.08 ± 1.89†

* $P < 0.05$ compared with 0.0 ppm.
† Dose response $P < 0.05$ based on regression analysis.

Table 4. *Volume Fraction (%) of Nonciliated Epithelial Cells in Tracheobronchial Airways of Rats Exposed to Ozone for 20 Months*

Airway	Region	Ozone concentration (ppm) 0.0	0.12	0.5	1.0
Distal trachea		42.4 ± 15.4	59.8 ± 25.6	46.7 ± 6.4	56.8 ± 4.1
Bronchus	Cranial	36.0 ± 13.6	26.3 ± 14.0	34.6 ± 7.7	41.4 ± 12.9
Bronchus	Central	35.5 ± 2.7	34.1 ± 11.2	28.0 ± 12.4	50.2 ± 16.7
Bronchus	Caudal	33.5 ± 3.9	24.5 ± 3.4	35.1 ± 15.8	43.4 ± 11.2

* $P < 0.05$ compared with 0.0 ppm.

were ciliated and basal, neither of which showed a significant change in relative abundance or cell mass.

Intrapulmonary Bronchi

Cranial

The bronchus in the cranial portion of the left lung (Figure 1A) was chosen for its short path length, small diameter, and large alteration in path angle from the trachea (Table 1). Carbohydrate histochemistry identified very few AB/PAS-positive inclusions in epithelial cells lining this airway in lungs of control animals. Most of the positively staining purplish material was observed in nonciliated cells (Figure 3). There was little difference in the distribution of AB/PAS-positive material in this airway generation in animals exposed to 0.12 or 0.5 ppm ozone compared with controls (Figure 4). However, in animals exposed to 1.0 ppm ozone, there was a marked increase in the amount of purplish-red to dark purple material observed in spherical and circular inclusions in nonciliated cells and an apparent increase in the number of cells containing AB/PAS-positive material (Figure 3).

The amount of AB/PAS-positive material stored in epithelial cells per unit area of basal lamina was over six times greater in this airway in animals exposed to 1.0 ppm ozone than it was in animals

Table 5. *Mass ($\mu m^3/\mu m^2$) Nonciliated Epithelial Cells in Tracheobronchial Airways of Rats Exposed to Ozone for 20 Months*

Airway	Region	Ozone concentration (ppm) 0.0	0.12	0.5	1.0
Distal trachea		3.15 ± 1.07	4.28 ± 1.12	3.82 ± 1.60	3.22 ± 0.60
Bronchus	Cranial	2.20 ± 1.03	1.71 ± 0.92	2.45 ± 0.95	2.92 ± 1.32
Bronchus	Central	1.89 ± 0.45	2.18 ± 0.98	1.43 ± 0.63	2.53 ± 0.73
Bronchus	Caudal	2.65 ± 0.90	1.92 ± 0.70	2.51 ± 1.26	2.10 ± 0.51

* $P < 0.05$ compared with 0.0 ppm.

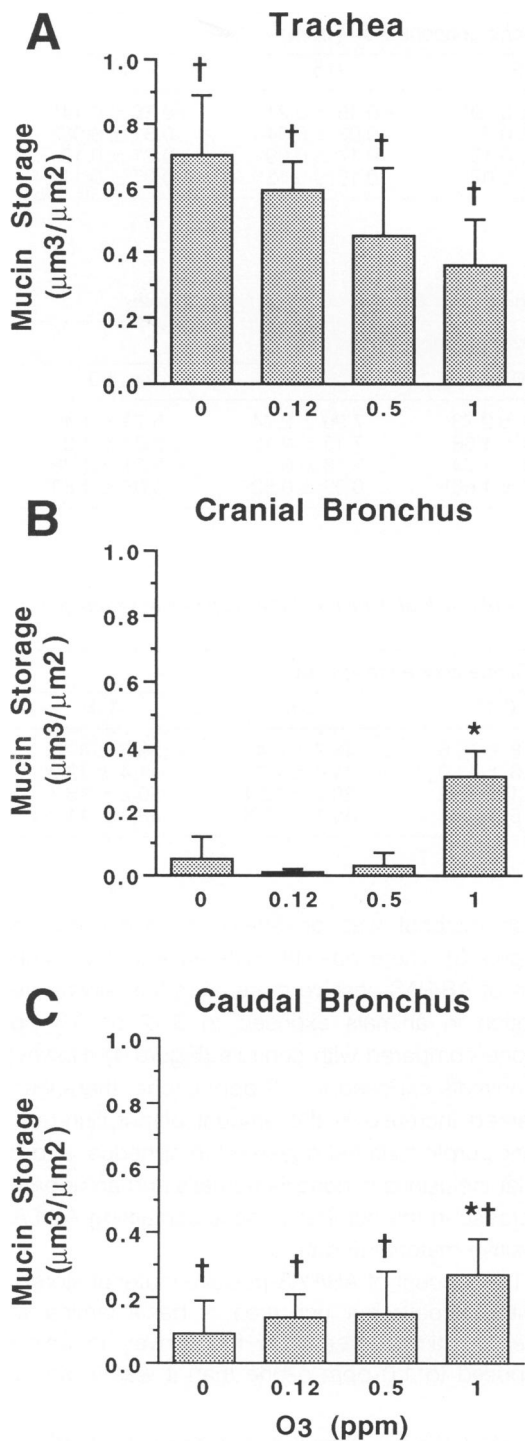

Figure 4. *Comparison of stored glycoconjugates in three regions in rats exposed for 20 months to filtered air or to 1.0 ppm ozone.* (**A**): *Trachea. Ozone exposure resulted in a dose-dependent loss of stored glycoconjugate in the trachea.* (**B**): *Cranial bronchus. Exposure to 1.0 ppm ozone significantly increased the amount of stored mucin in the cranial bronchus.* (**C**): *Caudal bronchus. Ozone exposure resulted in a dose-dependent increase of stored glycoconjugate in the caudal bronchus.* **Significantly different* ($P < 0.05$) *from filtered air control.* †*Significant* ($P < 0.05$) *dose response.*

exposed to filtered air or to lower ozone concentrations (Table 2, Figure 4). The histological appearance of the epithelial cells lining this airway in all exposure groups was not remarkably different (Figure 5). There were two categories of cells present: ciliated and nonciliated. There appeared to be some differences in the overall thickness of the epithelium in exposed groups, but ciliated cells with extensive cilia were clearly evident and the abundance of nonciliated cells was unchanged. Morphometric analysis of epithelium in the cranial bronchus indicated some increase in the total epithelial thickness (Table 3), in the proportion (volume fraction) of the epithelium composed of nonciliated cells (Table 4), and in the overall mass of nonciliated cells lining this airway (Table 5), but none of these differences was statistically significant. There was variability from animal to animal and within different regions of the same airway in an individual animal.

Central

The bronchus in the central portion of the left lung (Figure 1B) was selected for its short path length, large diameter, and small alteration in path angle from the trachea (Table 1). It was approximately the same path length from the carina as the cranial bronchus but had much less cumulative branch angle and over three times the cross-sectional diameter (Table 1). Carbohydrate histochemistry identified substantial amounts of AB/PAS-positive material in the nonciliated cells of this airway (Figure 3). There was approximately one-third as much AB/PAS-positive material stored in the nonciliated cells of this airway as in the trachea of control animals (Table 2). There appeared to be a small elevation in the amount of stored material in ozone-exposed animals but these differences were not statistically significant. The epithelium lining this airway was composed almost exclusively of nonciliated and ciliated cells varying in height from cuboidal to low columnar (Figure 5). The thickness of the epithelium (Table 3), the volume fraction of the epithelium composed of nonciliated cells (Table 4), and the mass of nonciliated cells per unit surface area were not significantly altered by ozone exposure (Table 5).

Caudal

The bronchus isolated from the caudal region (Figure 1C) was twice the number of generations of branching from the trachea as were the bronchi isolated from the cranial and central regions. This airway had a much longer path length from the carina,

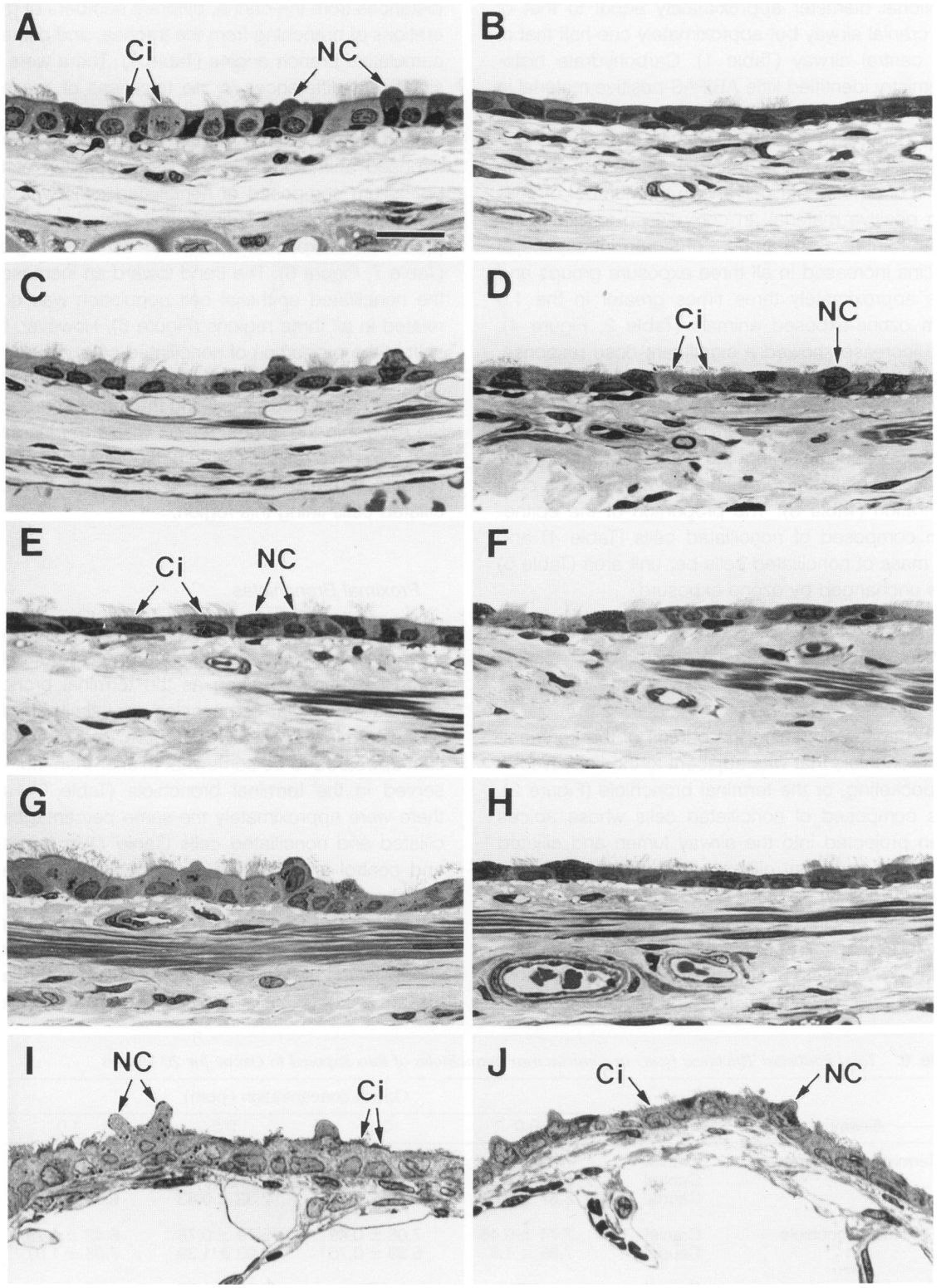

Figure 5. *Histopathological comparison of tracheobronchial epithelium in rats exposed for 20 months to filtered air (left column) or 1.0 ppm ozone (right column) (O_3). Toluidine blue. Bar = 20 μm.* (**A,B**): *Trachea.* (**C,D**): *Cranial bronchus.* (**E,F**): *Central bronchus.* (**G,H**): *Caudal bronchus.* (**I,J**): *Terminal bronchiole from caudal region in Figure 1.*

a low cumulative branch angle, and a cross-sectional diameter approximately equal to that of the cranial airway but approximately one-half that of the central airway (Table 1). Carbohydrate histochemistry identified little AB/PAS-positive material in the nonciliated cells lining this airway in control animals (Figures 3 and 4). However, in exposed animals, AB/PAS-positive material increased, both in terms of amount per cell and in the number of cells with positive material. In comparison to filtered air control animals, the amount of stored intraepithelial mucins increased in all three exposure groups and was approximately three times greater in the 1.0 ppm ozone-exposed animals (Table 2, Figure 4). This increase showed a significant dose response. The cellular composition of the epithelium lining this airway was similar to that observed in the cranial and central airways (Figure 5). The total thickness of the epithelium lining the caudal bronchus decreased significantly in relation to rising ozone concentration (Table 3). The proportion of the epithelium composed of nonciliated cells (Table 4) and the mass of nonciliated cells per unit area (Table 5) was unchanged by ozone exposure.

Central Acinus

Terminal Bronchioles

The epithelium lining the portion of the centriacinar bronchiole that was adjacent to the first alveolar outpocketing, or the terminal bronchiole (Figure 2), was composed of nonciliated cells whose apices often projected into the airway lumen and ciliated cells with abundant cilia on their luminal surfaces. The two cell types were also distinguished by the presence of cilia and basal bodies in the lightly staining cytoplasm of ciliated cells and the denser staining cytoplasm of secretory granules in the nonciliated cells (Figure 5). Terminal bronchioles were isolated from three separate regions with different distances from the carina, different numbers of generations of branching from the trachea, and different cumulative branch angles (Table 1). There were no significant differences in the thickness of this epithelium in any exposure groups except for a decrease in the cranial region of 1.0 ppm ozone-exposed animals (Table 6). The proportion of the epithelium composed of nonciliated cells was significantly elevated over filtered air controls in the 1.0 ppm ozone-exposed animals in all three regions (Table 7, Figure 6). The trend toward an increase in the nonciliated epithelial cell population was dose related in all three regions (Figure 6). However, this shift in the proportion of nonciliated cells did not result in a statistically significant increase in the total mass of nonciliated cells lining the terminal bronchiole except in the caudal region where the increase was also dose related (Table 8, Figure 6). There was no detectable AB/PAS-positive material in the nonciliated cells lining this region.

Proximal Bronchioles

The epithelium lining the bronchiole, which was approximately 1 mm closer to the trachea but in the same centriacinar region as the terminal bronchioles, had a cellular composition very similar to that of the terminal bronchioles (Figure 2). The epithelium appeared to be somewhat thicker than that observed in the terminal bronchiole (Table 6), and there were approximately the same percentages of ciliated and nonciliated cells (Table 7) in exposed and control animals. The mass of nonciliated epithelial cells was unchanged except for a significant decrease in the cranial region of the 1.0 ppm ozone-exposed animals (Table 8). There was some variability in the histological composition of this epithelium both within and between animals. There

Table 6. *Total Epithelial Thickness (μm) in Centriacinar Bronchioles of Rats Exposed to Ozone for 20 Months*

Airway	Region	Ozone concentration (ppm)			
		0.0	0.12	0.5	1.0
Terminal bronchiole	Cranial	7.03 ± 1.44	6.30 ± 0.33	6.89 ± 0.25	5.69 ± 0.74*
	Central	5.67 ± 0.22	8.23 ± 1.70	ND	6.55 ± 3.45
	Caudal	6.67 ± 0.61	7.72 ± 1.12	7.33 ± 0.83	6.99 ± 0.65
Proximal bronchiole	Cranial	7.71 ± 0.46	7.08 ± 0.49	6.79 ± 0.78	6.42 ± 1.79
	Caudal	7.85 ± 1.8	6.39 ± 0.75	6.93 ± 1.39	7.05 ± 1.07
Bronchiolar epithelium in alveolar ducts	Cranial	NP	NP	7.31 ± 1.27	6.72 ± 1.94
	Caudal	NP	NP	6.32 ± 1.74	7.29 ± 1.37

ND, not done; NP, not present.
* $P > 0.05$ compared with 0.0 ppm.

Table 7. *Volume Fraction (%) of Nonciliated Epithelial Cells in Centriacinar Bronchioles of Rats Exposed to Ozone for 20 Months*

Airway	Region	Ozone concentration (ppm)			
		0.0	0.12	0.5	1.0
Terminal bronchiole	Cranial	39.2 ± 10.8*	38.0 ± 3.9*	41.7 ± 6.8*	54.3 ± 10.3*†
	Central	29.6 ± 13.9*	44.9 ± 3.9*	ND	56.8 ± 18.4*†
	Caudal	36.1 ± 10.3*	44.2 ± 5.9*	54.2 ± 8.5*†	60.3 ± 6.5*†
Proximal bronchiole	Cranial	39.3 ± 5.2	31.4 ± 7.8	35.4 ± 13.4	34.2 ± 7.4
	Caudal	32.4 ± 13.5	38.2 ± 8.8	40.5 ± 11.0	46.4 ± 11.0
Bronchiolar epithelium in alveolar duct	Cranial	NP	NP	57.5 ± 8.5‡	59.5 ± 12.1‡
	Caudal	NP	NP	39.7 ± 8.6	57.8 ± 7.1‡

ND, not done, NP, not present.
* Dose response $P < 0.05$ based on regression analysis.
† $P < 0.05$ compared with same region in 0.0 ppm animals.
‡ $P < 0.05$ compared with terminal bronchiole in same region of 0.0 ppm animals.

Table 8. *Mass ($\mu m^3/\mu m^2$) of Nonciliated Epithelial Cells in Centriacinar Bronchioles of Rats Exposed to Ozone for 20 Months*

Airway	Region	Ozone concentration (ppm)			
		0.0	0.12	0.5	1.0
Terminal bronchiole	Cranial	2.66 ± 0.52	2.40 ± 0.35	2.87 ± 0.45	3.07 ± 0.61
	Central	1.69 ± 0.84	3.74 ± 1.02	ND	4.10 ± 3.16
	Caudal	2.38 ± 0.57*	3.44 ± 0.84*†	3.92 ± 0.17*†	4.21 ± 0.64*†
Proximal bronchiole	Cranial	3.04 ± 0.49	2.20 ± 0.39	2.41 ± 0.97	2.10 ± 0.14†
	Caudal	2.69 ± 1.70	2.44 ± 0.62	2.70 ± 0.33	3.22 ± 0.60
Bronchiolar epithelium in alveolar duct	Cranial	NP	NP	4.15 ± 0.42‡	3.88 ± 0.35‡
	Caudal	NP	NP	2.50 ± 0.94	4.23 ± 1.06‡

ND, not done; NP, not present.
* Dose response $P < 0.05$ based on regression analysis.
† $P < 0.05$ compared with same area in 0.0 ppm animals.
‡ $P < 0.05$ compared with terminal bronchiole in same region of 0.0 ppm animals.

was no detectable AB/PAS-positive material in the nonciliated cells lining this region.

Bronchiolar Epithelium in Alveolar Ducts

The centriacinar alveolar ducts of rats exposed to 0.5 and 1.0 ppm ozone had bronchiolar epithelium lining the luminal surfaces. This epithelium was composed of nonciliated cuboidal cells and ciliated cells (Figure 2). The epithelium lined not only the alveolar duct surface but also some of the alveolar outpocketings associated with this airway (Figure 2) and, in some cases, both sides of interalveolar septa. In animals exposed to filtered air, the epithelium lining these bronchiolarized alveolar ducts had approximately the same thickness as the epithelium lining the terminal bronchioles of the same regions (Table 6). The thickness was somewhat greater than in the terminal bronchioles of the same regions in ozone-exposed animals, but due to the variability from animal to animal, these differences were not statistically significant. The proportion of nonciliated cells in the bronchiolar epithelium in alveolar ducts was higher than in the terminal bronchioles of the same regions in control animals (Table 7). However, in only the caudal region of the 1.0 ppm ozone-exposed animals was this difference statistically significant.

The elevation in the caudal region in animals exposed to 0.5 ppm ozone was very small compared with the composition in the terminal bronchioles of the filtered air animals. The elevations in nonciliated cell proportion in alveolar ducts was not significantly different from that observed in the terminal bronchioles of the same animals. However, the mass of nonciliated cells in alveolar ducts was greater than that observed in terminal bronchioles of control animals (Table 8, Figure 7). The increase in nonciliated cell mass was similar to that observed in the terminal bronchioles of the same animals with the exception that there was more of an increase in the cranial region at 0.5 ppm than in the caudal region. Bronchiolar epithelium extended almost

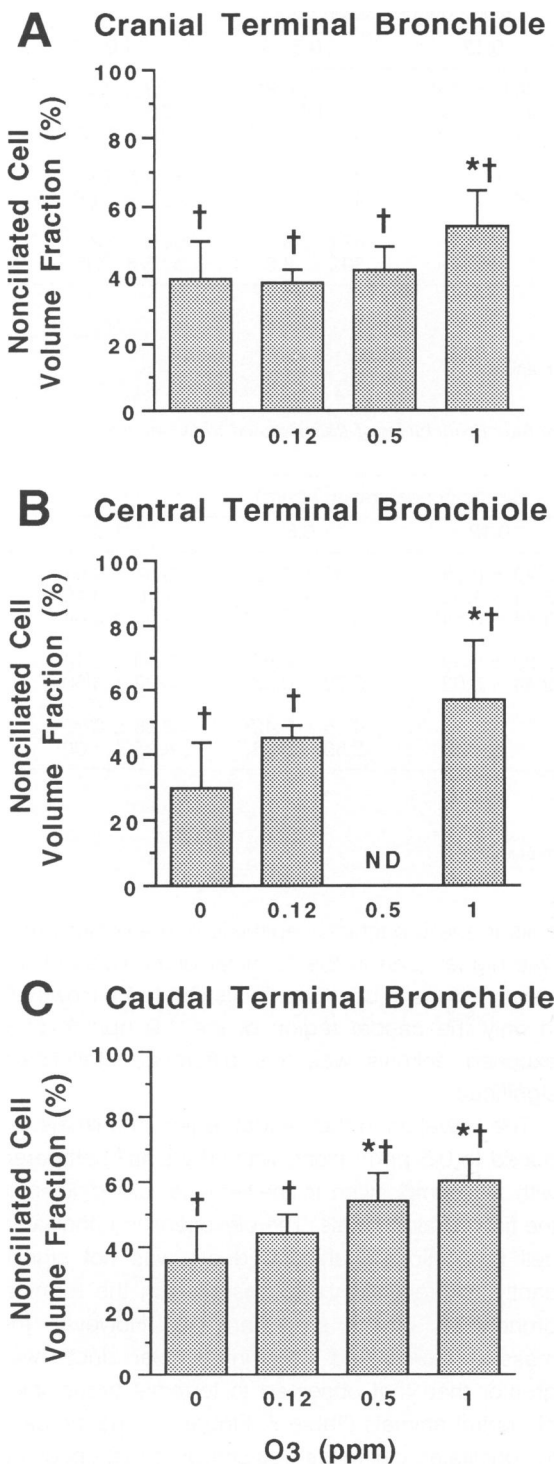

Figure 6. *Effects of ozone on the volume fraction (%) of nonciliated epithelial cells in terminal bronchioles.* (**A**): *Cranial terminal bronchiole.* (**B**): *Central terminal bronchiole.* (**C**): *Caudal terminal bronchiole. NP, not present.* **Significantly different* ($P < 0.05$) *from filtered air control.* †*Significant* ($P < 0.05$) *dose response.*

fourfold further into alveolar ducts in animals exposed to 1.0 ppm ozone than in controls (Figure 8). Both nonciliated and ciliated cells were found further into alveolar ducts in cranial regions than in caudal regions (Figure 8). There was no detectable AB/PAS-positive material in the nonciliated cells lining this region.

Discussion

This study tests the hypothesis that respiratory epithelium develops resistance to injury from oxidant air pollutants by reorganizing to favor cell types that show less susceptibility to the acute injury that results from initial exposure. We addressed this issue in animals exposed to the oxidant air pollutant ozone for nearly their life span. Because of the focal nature of the acute injury associated with ozone exposure, we attempted to characterize epithelial changes within carefully defined regions and to compare those changes in areas known to be highly susceptible to acute injury with changes in areas known to be less susceptible. Our results show that long-term exposure significantly alters the amount of secretory glycoconjugates stored in tracheobronchial epithelium. However, these alterations are site specific, both in terms of the direction of the change and of the exposure concentration required to elicit a change.

The cellular composition of the trachea and some proximal intrapulmonary conducting airways remained unaltered by ozone exposure. The airway generation that did show an increase in the amount of stored secretory product also sustained a loss in total cell mass, but did so without a significant change in epithelial composition. In contrast, in the centriacinar regions, the epithelium was significantly reorganized after ozone exposure. The primary change involved an increase in the proportion and total mass of nonciliated cells lining the terminal bronchioles. Proximal bronchiolar epithelium, which is not thought to be a major site of acute bronchiolar injury, was unaltered by the exposure conditions. The terminal bronchiolar epithelium of the centriacinar regions was reorganized in favor of the nonciliated cell population. The bronchiolar epithelium that lined bronchiolarized alveolar ducts in exposed animals exhibited a mixture of characteristics found in the terminal bronchiolar epithelial populations of both control and exposed animals. From this study, it appears that epithelial reorganization plays a role in the development of tolerance produced by long-term exposure to ozone. The

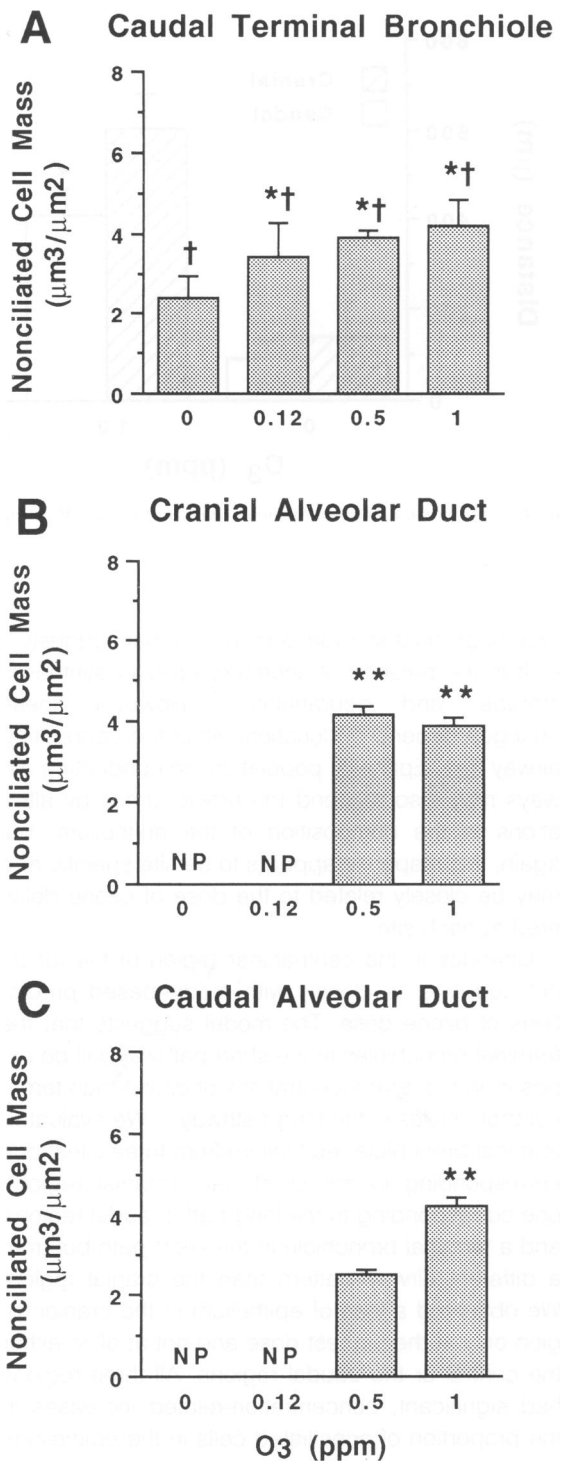

Figure 7. *Effects of ozone on the total mass of nonciliated epithelial cells in the caudal terminal bronchiole and the cranial and caudal alveolar ducts.* (**A**): *Caudal terminal bronchiole.* (**B**): *Cranial alveolar duct.* (**C**): *Caudal alveolar duct. NP, not present.* † *Significant* ($P < 0.05$) *dose response.* * *Significantly different* ($P < 0.05$) *from filtered air control.* ** *Significantly different* ($P < 0.05$) *from terminal bronchiole in filtered air controls.*

changes vary according to site and are most pronounced in those portions of the tracheobronchial tree that are most affected in short-term exposures. Some changes appear to be dose dependent, whereas others are not. The changes involve alterations in secretory activity and in the cellular composition of the epithelial lining.

The variability in epithelial response observed in different regions of the tracheobronchial airways is consistent with predictions of local ozone dose based on computer simulation models.[15–17] These models, which take into account differences in path length from the trachea to the terminal bronchiole, predict differences in the amount of ozone delivered to different sites within the tracheobronchial airways.[17] Our samples for evaluation were selected to correlate with the short pathway (distance from trachea to terminal bronchiole 7 to 8 generations of branching) and the long pathway (distance from trachea to terminal bronchiole 15 to 17 generations) used in those models. The changes in proximal conducting airways were primarily in stored secretory product and in composition of the epithelium. The bronchus we chose from the central region corresponds to the 4th to 6th generation bronchi in the long path in the ozone model. The dose of ozone to this site is predicted to be somewhat lower than in the trachea. Correspondingly, this airway showed no epithelial response to the long-term ozone exposure either in terms of altered secretory product storage or reorganized epithelial composition. There was, however, a shift toward an increasing proportion of nonciliated cells, but these changes were not statistically significant. Some of this shift may be due to the large variability that was observed in the epithelial response.

The model predicted a larger dose of ozone in more distal conducting airways of the same cross-sectional area in the long path (8 to 12 generations) than in the short path (4 to 5 generations). This prediction correlates with the differences in the amount of cellular change we observed in these two zones. The small diameter bronchus in the caudal zone or long path had a dramatic dose-dependent increase in the amount of stored secretory product and a dose-dependent decrease in total epithelial thickness. In the small diameter airway in the short path, the changes in stored secretory product were not nearly as dramatic and were observed only at the highest ozone concentration. There was no marked change in the thickness of the epithelium, which suggests that the changes in this airway were less severe than those in the airways of the same size but greater path length from the trachea. In con-

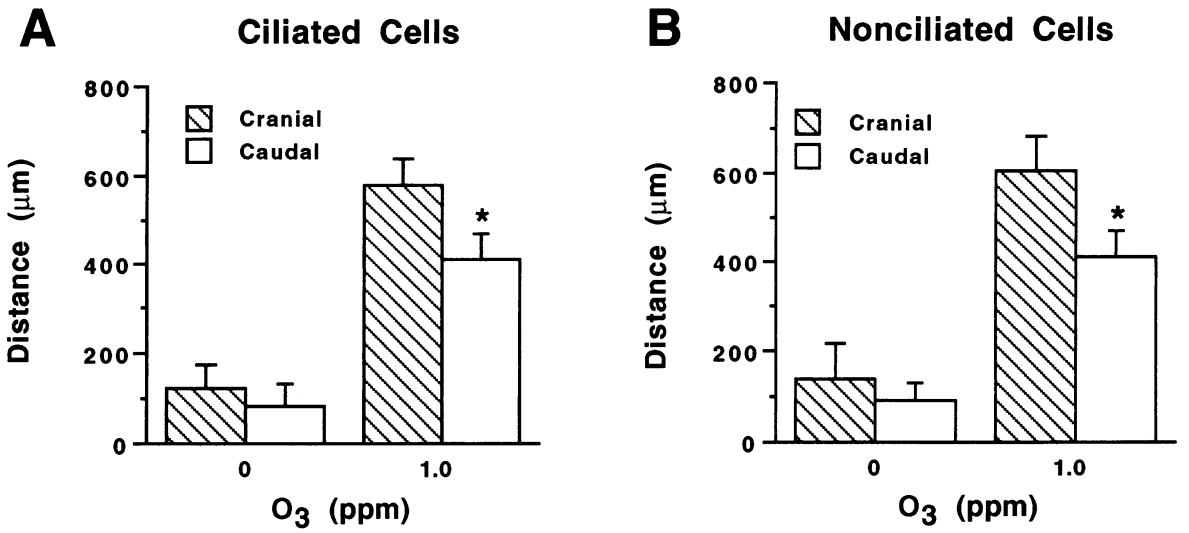

Figure 8. *Effects of ozone on the extent of bronchiolar epithelium into alveolar ducts in cranial and caudal regions.* (A): *Ciliated cells.* (B): *Nonciliated cells.* *$P < 0.05$ *compared with cranial region.*

trast, the principal change in the trachea, a site where ozone dose is predicted to be higher than in more distal conducting airways, was a concentration-related loss in stored secretory product.

Previous long-term (60-day exposures) studies, which have focused on the rat trachea, did not observe the same sorts of changes we had observed. In those studies, the secretory cell population and the amount of stored secretory product did not appear to change nor did the composition of the epithelial population.[18] There was, however, a loss of ciliated cells, a feature that we did not observe after 20 months. Long-term (1 year) exposure of rabbits to ozone at an ambient concentration (0.1 ppm) produced a transient (at 4 months) increase in secretory cell number, which was not present after 1 year.[7] In that study, analysis of epithelial responses to ambient concentrations of ozone (0.1 ppm) by airway size showed an increase in secretory cells in small and medium diameter airways but no change in larger airways. However, the lack of detectable change may be due to the high variability, which would be accounted for by not basing airway definition on position within the airway tree as predicted by models.

Short-term exposure studies have not found alterations in tracheobronchial mucous substances to be a major feature of the injury response in primates[19,20] or in rats.[21] It would appear then that part of the basic cellular response to chronic oxidant stress produced by long-term exposure to reactive gases such as ozone is an alteration in secretory product storage, a response that suggests a shift in the balance of secretory product synthesis, storage, and degranulation. However, these changes depend on location within the conducting airway tree. Epithelial populations in conducting airways may also respond to chronic stress by alterations in the composition of the epithelium, but again, this response appears to be site specific and may be closely related to the dose of ozone delivered at each site.

Changes in the centriacinar region of the rat do not correlate as closely with model-based predictions of ozone dose. The model suggests that the terminal bronchioles in the short pathway will be exposed to higher concentrations of ozone than terminal bronchioles in the long pathway.[17] We evaluated terminal bronchiolar epithelium from three sites: one corresponding to the short path (cranial region), one corresponding to the long path (caudal region), and a terminal bronchiole in the short path but from a different airway pattern than the cranial region. We observed a loss of epithelium in the cranial region only at the highest dose and not at all in either the central or the caudal regions. All three regions had significant, concentration-related increases in the proportion of nonciliated cells in the epithelium. However, in only one case (caudal region) was there actually a significant elevation in the total mass of nonciliated cells present. This finding suggests that epithelium in terminal bronchioles responds differently to ozone exposure depending on its position within the tree, but other factors, in addition to the predicted ozone dose, may also be im-

portant. Two such factors that may account for increased injury to terminal bronchioles in the long path may be that: 1) in our case, the long path was located in the caudal region, a zone that could receive a larger volume of air, and hence ozone, during inspiration or 2) ventilatory unit size is greater in the caudal region. Either of these factors would result in a higher ozone dose to that region than predicted.[22–24] The model predicts that regardless of path the lowest concentration of ozone throughout the conducting airways will be in the airway one generation proximal to the terminal bronchiole.[17] We evaluated this site in two regions, short path (cranial region) and long path (caudal region). As predicted, we found minimal change as a result of ozone exposure.

We also evaluated the epithelium that lines bronchiolarized alveolar ducts. In our previous study,[5] ozone exposure was found to cause a significant extension of bronchiolar epithelium into alveolar ducts. This study addresses whether the epithelial composition in these bronchiolarized zones has the same characteristics as the populations in terminal bronchioles. We found that the bronchiolar population in alveolar ducts is most similar to that observed in the terminal bronchioles of ozone-exposed animals. The total mass of epithelium was not significantly different from that observed in the terminal bronchioles of controls of the same region, but the proportion and total mass of nonciliated cells were significantly greater than in terminal bronchioles of control animals and more closely matched the conditions in the terminal bronchioles from the same regions of exposed animals. There was also marked increase in the distance that bronchiolar epithelium extended into alveolar ducts in exposed animals, with the distance being significantly further in the cranial region, where the pathway is shorter and the predicted dose higher, than in the caudal region.

In summary, the study shows that the epithelial populations in conducting airways, which are targets for injury in initial phases of inhalation of reactive oxidant gases, establish a new homeostasis in which cell injury is no longer an obvious result of exposure. Epithelial populations establish a variety of new conformations directly associated with the development of tolerance. These conformations involve alterations in secretory product storage and shifts in epithelial composition toward cell types that are less susceptible to acute injury. It appears that long-term, essentially lifetime exposure to injurious oxidant gases cause the epithelium to be redefined. In addition to ozone, repeated exposure to nitrogen dioxide results in nonciliated cell hyperplasia in central acinar bronchioles.[25] Long-term exposure to a number of other irritants, including sulfur dioxide, sulfuric acid aerosol, cigarette smoke, and formaldehyde, produce secretory cell hyperplasia in the proximal respiratory tract.[7,26–29] However, as our study shows, this redefinition, at least for ozone, depends on the specific location of the epithelium and probably also its local microenvironment and preexposure composition. Epithelial cells lining the trachea respond differently to chronic injury than epithelial cells lining more distal conducting airways. In addition, the response in terminal bronchioles, another major site of injury, is different from that observed in more proximal airways. Finally, all of the regional differences in the epithelial response correlate closely with the predicted ozone dose at those sites.

Acknowledgments

Research described in this article was conducted under contract to HEI, an organization jointly funded by the U.S. Environmental Protection Agency (Assistance Agreement X-816285) and automotive manufacturers. The contents of this article do not necessarily reflect the views of HEI, nor do they necessarily reflect the policies of the Environmental Protection Agency or automotive manufacturers. Animals were exposed as part of a NTP/HEI collaborative effort. The exposures were done at Battelle, Pacific Northwest Laboratories under contract to NTP.

We thank Dr. Debra A. Kaden of HEI for coordination and planning efforts, Dr. Paul W. Mellick of Battelle (Pacific Northwest Laboratories), and Dr. Gary A. Boorman of NTP during the course of this study. We also thank Diane Cranz for technical editing and Susan Nishio and Alison Weir for preparing the figures. U.C. Davis is an NIEHS Center for Environmental Health Sciences (ES05707).

References

1. Boorman GA, Schwartz LW, Dungworth DL: Pulmonary effects of prolonged ozone insult in rats: morphometric evaluation of the central acinus. Lab Invest 1980, 43: 108–115
2. Penha PD, Werthamer S: Pulmonary lesions induced by long-term exposure to ozone. II. Ultrastructure observations of proliferative and regressive lesions. Arch Environ Health 1974, 29:282–289
3. Barr BC, Hyde DM, Plopper CG, Dungworth DL: Distal airway remodeling in rats chronically exposed to

ozone. Am Rev Respir Dis 1988, 137:924–938
4. Barr BC, Hyde DM, Plopper CG, Dungworth DL: A comparison of terminal airway remodeling in chronic daily versus episodic ozone exposure. Toxicol Appl Pharmacol 1990, 106:384–407
5. Pinkerton KE, Dodge DE, Cederdahl-Demmler J, Wong VJ, Peake J, Haselton CJ, Mellick PW, Singh G, Plopper CG: Differentiated bronchiolar epithelium in alveolar ducts of rats exposed to ozone for 20 months. Am J Pathol 1993, 142:947–956
6. Hyde DM, Hubbard WC, Wong V, Wu R, Pinkerton K, Plopper CG: Ozone-induced acute tracheobronchial epithelial injury: relationship to granulocyte emigration in the lung. Am J Respir Cell Mol Biol 1992, 6:481–497
7. Schlesinger RB, Gorczynski JE, Dennison J, Richards L, Kinney PL, Bosland MC: Long-term intermittent exposure to sulfuric acid aerosol, ozone, and their combination: alterations in tracheobronchial mucociliary clearance and epithelial secretory cells. Exp Lung Res 1992, 18:505–534
8. Plopper CG: Structural methods for studying bronchiolar epithelial cells. Models of lung disease: microscopy and structural methods. Edited by J Gil. New York, Marcel Dekker, Inc., 1990, pp 537–559
9. Phalen RF, Oldham MJ: Tracheobronchial airway structure as revealed by casting techniques. Am Rev Respir Dis 1983, 128:51–53
10. Phalen RF, Yeh HC, Schum GM, Raabe OG: Application of an idealized model to morphometry of the mammalian tracheobronchial tree. Anat Rec 1978, 190:167–176
11. Hyde DM, Plopper CG, St. George JA, Harkema JR: Morphometric cell biology of air space epithelium. Electron microscopy of the lung. Edited by DE Schraufnagel. New York, Marcel Dekker, Inc., 1990, pp 1–120
12. Hyde DM, Magliano DJ, Plopper CG: Morphometric assessment of pulmonary toxicity in the rodent lung. Toxicol Pathol 1992, 19:428–446
13. Plopper CG, Macklin J, Nishio SJ, Hyde DM, Buckpitt AR: Relationship of cytochrome P450 activity to Clara cell cytotoxicity. III. Morphometric comparison of changes in the epithelial populations of terminal bronchioles and lobar bronchi in mice, hamsters, and rats after parenteral administration of naphthalene. Lab Invest 1992, 67:553–565
14. Dowdy S, Wearden S: Statistics for research. New York, J. Wiley and Sons, 1983, p 537
15. Overton JH, Graham RC, Miller FJ: A model of the regional uptake of gaseous pollutants in the lung. II. The sensitivity of ozone uptake in laboratory animal lungs to anatomical and ventilatory parameters. Toxicol Appl Pharmacol 1987, 88:418–432
16. Miller FJ, Overton JH, Gerrity TR, Graham RC: Interspecies dosimetry of reactive gases. Inhalation toxicology. Edited by U Mohr. New York, Springer-Verlag, 1988, pp 139–155
17. Overton JH, Barnett AE, Graham RC: Significances of the variability of tracheobronchial airway paths and their air flow rates to dosimetry model predictions of the absorption of gases. Extrapolation of dosimetric relationships for inhaled particles and gases. Edited by JD Crapo. New York, Academic Press, Inc., 1989, pp 273–291
18. Nikula KJ, Wilson DW, Giri S, Plopper CG, Dungworth DL: The response of the rat tracheal epithelium to ozone exposure: injury, adaptation, and repair. Am J Pathol 1988, 131:373–384
19. Wilson DW, Plopper CG, Dungworth DL: The response of the macaque tracheobronchial epithelium to acute ozone injury. Am J Pathol 1984, 116:193–206
20. Mellick PW, Dungworth DL, Schwartz LW, Tyler WS: Short-term morphologic effects of high ambient levels of ozone on lungs of rhesus monkeys. Lab Invest 1977, 36:82–90
21. Schwartz LW, Dungworth DL, Mustafa MG, Tarkington BK, Tyler WS: Pulmonary responses of rats to ambient levels of ozone: effects of 7-day intermittent or continuous exposure. Lab Invest 1976, 34:565–578
22. Mercer RR, Crapo JD: Three-dimensional reconstruction of the rat acinus. J Appl Physiol 1987, 63:785–794
23. Mercer RR, Pinkerton KE: The influence of ventilatory unit size on the distribution and uptake of reactive gases. Biofluid mechanics. Edited by DJ Schneck, CL Lucas. New York, New York University Press, 1990, pp 27–35
24. Mercer RR, Crapo JD: Architecture of the Acinus. Treatise on pulmonary toxicology: comparative biology of the normal lung. Edited by RA Parent. Boca Raton, FL, CRC Press, 1991, pp 109–119
25. Evans MJ, Shami SG, Cabral-Anderson LJ, Dekker NP: Role of nonciliated cells in renewal of the bronchial epithelium of rats exposed to NO_2. Am J Pathol 1986, 123:126–133
26. Lamb D, Reid L: Mitotic rates, goblet cell increase and histochemical changes in mucus in rat bronchial epithelium during exposure to sulphur dioxide. J Pathol Bacteriol 1968, 96:97–111
27. Lamb D, Reid L: Goblet cell increase in rat bronchial epithelium after exposure to cigarette and cigar tobacco smoke. Br Med J 1969, 1:33–35
28. Spicer SS, Chakrin LW, Wardell JR: Effect of chronic sulfur dioxide inhalation on the carbohydrate histochemistry and histology of the canine respiratory tract. Am Rev Respir Dis 1974, 110:13–24
29. Ionescu J, Marinescu D, Tapu V, Eskanasy A: Experimental chronic exposure to formaldehyde. Morphol Embryol 1978, 24:233–242